Enhanced thermodynamic stability of tetragonal-phase field in epitaxial Pb(Zr,Ti)O 3 thin films under a two-dimensional compressive stress

S. Hoon Oh and Hyun M. Jang

Articles you may be interested in

Two-dimensional mapping of triaxial strain fields in a multiferroic Bi Fe O 3 thin film using scanning x-ray microdiffraction
Appl. Phys. Lett. **90**, 102904 (2007); 10.1063/1.2711530

Lattice strain in epitaxial Ba Ti O 3 thin films
Appl. Phys. Lett. **88**, 152908 (2006); 10.1063/1.2194231

Morphotropic phase boundary in epitaxial Pb (Zr , Ti) O 3 thin films: Two-dimensional planar size effect
Appl. Phys. Lett. **86**, 202901 (2005); 10.1063/1.1925315

Thermodynamic theory of stress distribution in epitaxial Pb(Zr,Ti)O 3 thin films
Appl. Phys. Lett. **75**, 3195 (1999); 10.1063/1.125275

Reciprocal space mapping of phase transformation in epitaxial PbTiO 3 thin films using synchrotron x-ray diffraction
J. Appl. Phys. **85**, 1995 (1999); 10.1063/1.369195

Enhanced thermodynamic stability of tetragonal-phase field in epitaxial Pb(Zr,Ti)O$_3$ thin films under a two-dimensional compressive stress

S. Hoon Oh and Hyun M. Jang
Department of Materials Science and Engineering, and Laboratory for Physics/Chemistry of Dielectric Materials, Pohang University of Science and Technology (POSTECH), Pohang 790-784, Korea

A two-dimensional thermodynamic model was developed to account for the observed difficulty in the fabrication of epitaxial Pb(Zr,Ti)O$_3$ (PZT) thin films in which tetragonal and rhombohedral phases coexist. The thermodynamic formalism based on the Landau–Devonshire's phenomenological theory predicts the enhanced thermodynamic stability of the tetragonal-phase field under a two-dimensional compressive stress. We have experimentally proved this prediction by fabricating an epitaxially oriented tetragonal PZT thin film on MgO substrate with the target composition corresponding to the bulk morphotropic phase boundary (MPB). © *1998 American Institute of Physics.* [S0003-6951(98)02412-7]

Up to date, extensive efforts have been made for the fabrication of epitaxially oriented Pb(Zr,Ti)O$_3$ (PZT) thin films in which tetragonal and rhombohedral phases coexist with each other.[1–3] Bulk polycrystalline PZT ceramics having the two-coexisting-phases can be easily fabricated by adjusting the ratio of Zr to Ti to near 52:48. A bulk PZT specimen in the vicinity of this composition is characterized by the morphotropic phase boundary (MPB) on which the two phases coexist without the solubility gap (not obeying the lever rule).[4] Let us call this composition as the bulk MPB composition (i.e., Zr:Ti≈52/48). Polycrystalline PZT ceramics usually exhibit their maximum values of the relative dielectric permittivity and the electromechanical coupling coefficient in the vicinity of the MPB.[5] Therefore, a great deal of effort has been made to obtain an epitaxially oriented PZT thin film in which the two phases coexist. Until now, however, these attempts have not been successful even with the compositions near the MPB.[1–3]

In this letter, we have examined the reason behind the observed difficulty in the fabrication of the epitaxial PZT thin film in which the two phases coexist and developed a two-dimensional thermodynamic model for epitaxial ferroelectric thin films. This formulation based on the Landau–Devonshire's phenomenological theory predicts an extension of the tetragonal-phase field under a two-dimensional compressive stress. We have experimentally proved this prediction by fabricating an epitaxially oriented tetragonal PZT thin film on MgO substrate with the target composition corresponding to the bulk MPB composition.

Applications of the Landau–Devonshire's phenomenological thermodynamic formalism to ferroelectric perovskites revealed that a stress could be very effective in displacing the MPB in the PZT system[6] and that the ferro-para transition temperature of the PbTiO$_3$ thin film was increased by a two-dimensional compressive stress.[7] Therefore, one does expect that a two-dimensional compressive stress with its direction perpendicular to the c axis can give rise to the shift of both the MPB and the transition temperature (T_c) in the epitaxially oriented PZT films. If the thickness of the substrate is much greater than that of the film and a thermal stress (σ) is uniformly developed throughout the film, the magnitude of the thermal stress exerted on the epitaxially grown film can be estimated using the following relation:[8]

$$\sigma = (a_s - a_f)/(s_{11} + s_{12})\Delta T, \tag{1}$$

where a_s and a_f, respectively, are the linear coefficients of thermal expansion for the substrate and the film, s_{11}, s_{12} are the elastic compliances of the film, and ΔT is the temperature difference. We have estimated the thermal stress using the following values:[5,6,9] $s_{11} = 6.785 \times 10^{-12}$ m^2/N, $s_{12} = -2.5 \times 10^{-12}$ m^2/N, $a_s = 13.3 \times 10^{-6}$ °C^{-1} (for MgO), $a_f = 9.0 \times 10^{-6}$ °C^{-1} (for PZT). This type of simple calculation suggests that the thermal expansion mismatch between the PZT film and the MgO substrate can result in a large net compressive stress (~ 1.0 MPa/°C).

We will use the phenomenological thermodynamic formalism to show directly that a two-dimensional stress not only provokes the shift of the MPB in the epitaxial PZT thin films but also forces them to be in the tetragonal-phase field. For this purpose, we first consider the elastic Gibbs function in the absence of antiferroelectric polarizations and oxygen octahedral tiltings:[10]

$$\Delta G = \alpha_1(P_1^2 + P_2^2 + P_3^2) + \alpha_{11}(P_1^4 + P_2^4 + P_3^4) + \alpha_{12}(P_1^2 P_2^2 + P_2^2 P_3^2 + P_3^2 P_1^2) + \alpha_{111}(P_1^6 + P_2^6 + P_3^6)$$

$$+ \alpha_{112}[P_1^4(P_2^2 + P_3^2) + P_2^4(P_3^2 + P_1^2) + P_3^4(P_1^2 + P_2^2)] + \alpha_{123}P_1^2 P_2^2 P_3^2 - 1/2 s_{11}(X_1^2 + X_2^2 + X_3^2)$$

$$- s_{12}(X_1 X_2 + X_2 X_3 + X_3 X_1) - 1/2 s_{44}(X_4^2 + X_5^2 + X_6^2) - Q_{11}(X_1 P_1^2 + X_2 P_2^2 + X_3 P_3^2)$$

$$- Q_{12}[X_1(P_2^2 + P_3^2) + X_2(P_3^2 + P_1^2) + X_3(P_1^2 + P_2^2)] - Q_{44}(X_4 P_2 P_3 + X_5 P_3 P_1 + X_6 P_1 P_2), \tag{2}$$

where P_i is the magnitude of the polarization vector along the direction i, α_i is the dielectric stiffness, α_{ij}, α_{ijk} are the high-order stiffness coefficients at constant stress, s_{11}, s_{12}, s_{44} are the elastic compliances measured at constant polarization, and Q_{11}, Q_{12}, Q_{44} are the electrostrictive coefficients written in polarization notation. In the reduced notation, X_1, X_2, X_3 denote the tensile stresses and X_4, X_5, X_6 the shear components. The dielectric stiffness constant, α_1, is assumed to be a linear function of temperature near the Curie temperature (the Curie–Weiss law). All other coefficients are assumed to be independent of temperature, and their optimized values are given in a series of papers reported by Haun and co-workers.[10,11]

We are now considering the elastic Gibbs function in the presence of a two-dimensional compressive stress. The following relations hold under this condition:

$$X_1 = X_2 = -\sigma, \quad X_3 = X_4 = X_5 = X_6 = 0, \tag{3}$$

where the negative sign signifies a compressive stress. Using the partial derivative of ΔG with respect to P_i in the absence of any external field (i.e., $\partial \Delta G/\partial P_i = E_i = 0$) one can derive the following relations for the spontaneous polarization and the elastic Gibbs free energy:

Cubic Phase:

$$P_1^2 = P_2^2 = P_3^2 = 0,$$
$$\Delta G = -(s_{11} + s_{12})\sigma^2. \tag{4}$$

Tetragonal Phase:

$$P_3^2 = P_s^2 = \frac{-\alpha_{11} + [\alpha_{11}^2 - 3\alpha_{111}(\alpha_1 + 2Q_{12}\sigma)]^{1/2}}{3\alpha_{111}},$$
$$P_1^2 = P_2^2 = 0,$$
$$\Delta G = -(s_{11} + s_{12})\sigma^2 + (\alpha_1 + 2Q_{12}\sigma)P_3^2 + \alpha_{11}P_3^4$$
$$\quad + \alpha_{111}P_3^6. \tag{5}$$

Rhombohedral Phase:

$$P_1^2 = P_2^2 = P_3^2 = P_s^2 = \frac{-(\alpha_{11} + \alpha_{12}) + [(\alpha_{11} + \alpha_{12})^2 - 1/3(3\alpha_{111} + 6\alpha_{112} + \alpha_{123})(3\alpha_1 + 2\sigma Q_{11} + 4\sigma Q_{12})]^{1/2}}{3\alpha_{111} + 6\alpha_{112} + \alpha_{123}},$$
$$\Delta G = -(s_{11} + s_{12})\sigma^2 + (3\alpha_1 + 2Q_{11}\sigma + 4Q_{12}\sigma)P_3^2 + 3(\alpha_{11} + \alpha_{12})P_3^4 + (3\alpha_{111} + 6\alpha_{112} + \alpha_{123})P_3^6. \tag{6}$$

Imposing the condition that $\Delta G_{tet} = \Delta G_{rhom}$ at the MPB and that $\Delta G_{cubic} = \Delta G_{rhom}$ or $\Delta G_{cubic} = \Delta G_{tet}$ at the transition temperature (T_c), one can simulate phase diagrams for a given value of the compressive stress. Figure 1 shows the effect of compressive stress (50 MPa) on the shift of the MPB and the transition temperature. As shown in Fig. 1, at a given temperature the MPB moves toward the rhombohedral-phase fie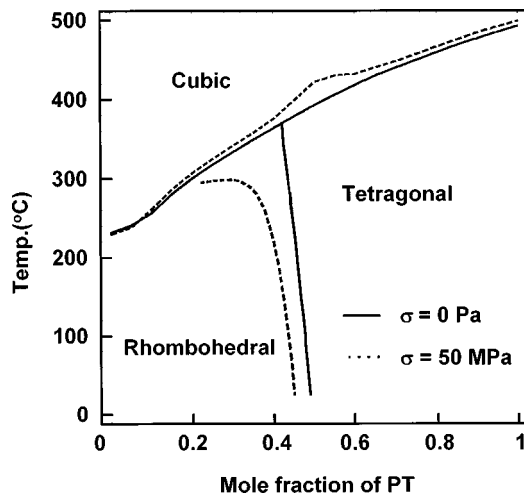ld as the applied compressive stress increases. This tendency increases with increasing temperature so as to make the cubic-tetragonal phase transition possible even though the rhombohedral phase is more stable at room temperature.

From the above results, it can be said that the stability of the tetragonal-phase field is enhanced by the presence of the compressive stress. Thus it is expected that, unlike bulk polycrystalline ceramics, the teragonal phase will not coexist with the rhombohedral phase even at the bulk MPB composition when a two-dimensional compressive stress is effective on the epitaxial PZT thin film.

In order to experimentally verify this prediction we have prepared PZT thin films using a radio-frequency magnetron sputtering system and investigated their crystal structure. The chemical composition of the target used in the present study is $Pb_{1.1}(Zr_{0.52}Ti_{0.48})O_3$. An excess amount of Pb was used to obtain a film composition close to the desired stoichiometry. The sputtering conditions employed in the present study are summarized in Table I. The deposited films were annealed on the substrate heater at 650 °C in air ambient to stabilize perovskite phase and to minimize other stress effects except for a thermal stress.

FIG. 1. The computed phase diagram of $PbZrO_3$-$PbTiO_3$ pseudo-binary system, showing the effect of two-dimensional compressive stress on the shift of the MPB and T_c. The solid lines represent the MPB and T_c in the absence of the compressive stress. On the other hand, the dotted lines correspond to those under the stress.

TABLE I. Sputtering conditions.

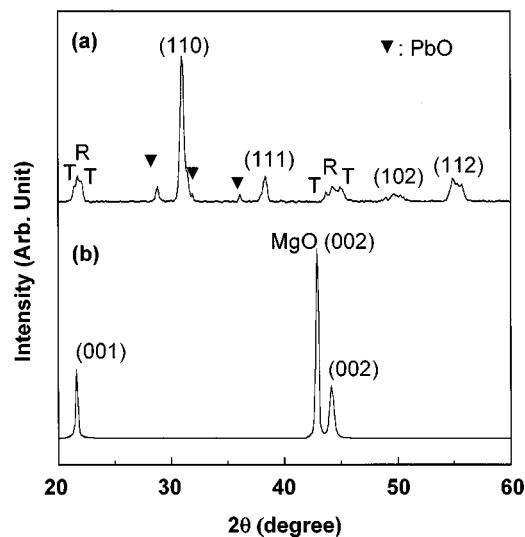|	
RF power	40 W
Sputtering gas	Ar/O_2 (90/10)
Gas pressure	1.2×10^{-2} Torr
Substrate temperature	520 °C
Target-substrate distance	80 mm

FIG. 2. XRD patterns of the PZT target and the thin film: (a) target specimen with the composition $Pb_{1.1}(Zr_{0.52}Ti_{0.48})O_3$, (b) thin film deposited on (001) MgO single crystal.

FIG. 3. X-ray Φ scan diffraction spectra of (a) PZT (56/44) thin film and (b) MgO substrate.

The chemical composition of the film was investigated as choosing its target to be a reference sample. Energy dispersive x-ray (EDX) spectroscopy analysis showed that the Zr/Ti ratio (56/44) of the film was slightly larger than that of the target (Zr/Ti=52/48). The x-ray diffraction (XRD) patterns (with Cu K_α radiation) of the PZT thin film and the target are shown in Fig. 2. As indicated in the figure, only the (001) and (002) PZT reflections along with the (002) substrate reflection are visible in the film [Fig. 2(b)] without any peak splitting into c or a axis. On the other hand, all of the relevant PZT peaks that are originated from the coexistence of the tetragonal phase with the rhombohedral symmetry are visible in the bulk ceramics having the target composition [Fig. 2(a)]. Therefore, the XRD patterns indicate that there exists only one crystalline structure in the PZT film prepared from the bulk MPB composition (i.e., Zr/Ti=52/48). The XRD analysis also suggests that its interplanar spacing perpendicular to the MgO substrate is 4.09 Å.

To examine the orientational relationship and the epitaxial growth we have performed Φ scans on the MgO(200) and the PZT(200) planes. For this purpose, we did the x-ray θ-2θ scan on the MgO(200) plane first and detected a (200) MgO peak at $2\theta=42.91°$ and a (200) PZT peak at $2\theta=44.48°$. Thus, the PZT(200) planes are almost parallel to the MgO(200) planes. For a more precise measurement, we subsequently did the θ rocking at $2\theta=44.48°$ and found that the PZT(200) was tilted about 0.3° with respect to the MgO(200). After adjusting the theta (θ) for a precise Bragg diffraction condition, 2θ was remeasured for the PZT(200) reflection. This acquainted us that its interplanar spacing was about 4.07 Å. Figure 3 shows the x-ray Φ scan spectra for the (200) reflections [$2\theta=42.91°$ for (200) MgO and $2\theta=44.52°$ for (200) PZT]. These peaks occur nearly at the same azimuthal Φ angles as the substrate reflections and are observed 90° apart. This is caused by the four-fold symmetry of the specimen which is epitaxially grown as ''cube on cube.''

The above experimental results clearly demonstrate that the PZT film deposited on the MgO(001) substrate is epitaxi-
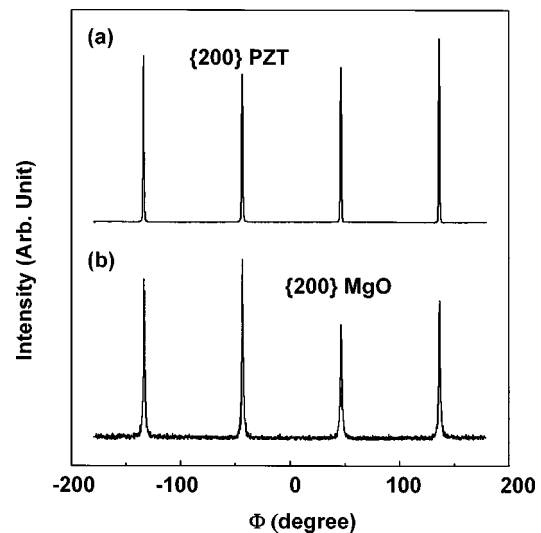
ally grown as PZT(001)//MgO(001). It also reveals that, due to a compressive thermal stress, the PZT film has a tetragonal structure in which the c-axis lattice constant is found to be about 4.09 Å and the a axis about 4.07 Å. The estimated c-axis lattice constant is smaller than the reported value of the c axis for the target PZT (4.13 Å). On the other hand, the a-axis lattice constant is slightly larger than that for the bulk target specimen (4.04 Å). Since the c/a ratio decreases with increasing Zr/Ti ratio in the PZT, the observed discrepancies can be attributed to the larger Zr/Ti ratio of the film (56/44) compared to that of the target (52/48).

In conclusion, the phenomenological thermodynamic model presented in this letter indicates that an epitaxial PZT film under a sufficiently large two-dimensional compressive stress should be tetragonal even though its composition (Zr/Ti≈56/44) corresponds to the rhombohedral phase field in a polycrystalline form. This prediction was experimentally confirmed by analyzing the structure of the PZT film fabricated on the MgO(001) substrate.

[1] R. Takayama and Y. Tomita, J. Appl. Phys. **65**, 1666 (1989).
[2] J. Lee, S. Esayan, J. Prohaska, and A. Safari, Appl. Phys. Lett. **64**, 294 (1994).
[3] I. Kanno, S. Hayashi, T. Kamada, M. Kitagawa, and T. Hirao, Jpn. J. Appl. Phys., Part 1 **33**, 574 (1994).
[4] W. Cao and L. E. Cross, Phys. Rev. B **47**, 4825 (1993).
[5] B. Jaffe, W. R. Cook, Jr., and H. Jaffe, *Piezoelectric Ceramics* (Academic, New York, 1971).
[6] A. Amin, R. E. Newnham, and L. E. Cross, Phys. Rev. B **34**, 1595 (1986).
[7] G. A. Rossetti, Jr., L. E. Cross, and K. Kushida, Appl. Phys. Lett. **59**, 2524 (1991).
[8] M. Ohring, *The Materials Science of Thin Films* (Academic, London, 1992).
[9] G. V. Samsonov, *The Oxide Handbook*, 2nd ed. (IFI/Plenum Data Company, New York, 1982).
[10] M. J. Haun, E. Furman, S. J. Jang, and L. E. Cross, Ferroelectrics **99**, 13, Parts I, II, III, IV, and V (1989).
[11] M. J. Haun, Z. Q. Zhuang, E. Furman, S. J. Jang, and L. E. Cross, J. Am. Ceram. Soc. **72**, 1140 (1989).